Available online at www.sciencedirect.com
SCIENCE DIRECT®
Journal of Catalysis 221 (2004) 432–440
JOURNAL OF CATALYSIS
www.elsevier.com/locate/jcat

Effects of sol–gel procedures on the photocatalysis of Cu/TiO_2 in CO_2 photoreduction

I-Hsiang Tseng, Jeffrey C.S. Wu,* and Hsin-Ying Chou

Department of Chemical Engineering, National Taiwan University, Taipei 10617, Taiwan, Republic of China

Received 28 January 2003; revised 27 August 2003; accepted 3 September 2003

Abstract

Copper-loaded titania (Cu/TiO_2) was synthesized via an improved modified sol–gel process. Photocatalysts were applied to the CO_2 photocatalytic reduction and the yield of the major product, methanol, was used to evaluate the photocatalytic performance. Copper precursors and the adding time with sol as well as posttreatments were studied to explore the relationships between the characteristics and the activity of the photocatalysts. The results revealed that Cu/TiO_2 prepared from copper chloride and added in the early sol–gel stage was more photoactive than that from copper acetate. Additional H_2 reduction of calcined catalysts before the photoreduction CO_2 decreased the yield of methanol due to the change of copper dispersion and oxidation state. TPR, XPS, and XAS measurements verified the oxidation state of Cu on Cu/TiO_2 catalysts. The results indicated that the primary Cu(I) served as an active site. The zeta potentials of catalysts were measured and compared, showing that a higher positive zeta potential at pH 7 would lead to higher activity. Under 30-h UVC (254 nm) irradiation, the best catalyst gave a methanol yield above 600 $\mu mol/g_{cat}$. Switching to UVA (365 nm) resulted in a significant decrease of methanol yield in the range of 10 $\mu mol/g_{cat}$.

Keywords: Cu/TiO_2; CO_2; Photoreduction; XANES; EXAFS; Sol–gel

1. Introduction

The sol–gel process is suitable for producing composite materials of high purity without multiple steps. In previous work [1], homogeneous, nano-sized, copper-loaded anatase titania was synthesized by the improved sol–gel method. These titania photocatalysts were applied to the photoreduction of carbon dioxide in order to evaluate their photocatalytic performance. Methanol was found to be the primary hydrocarbon product [2].

Various methods exist for solving the problem of the greenhouse gas, carbon dioxide, on earth. One permanent solution is to transfer it chemically into a useful and nontoxic material. Several studies [3–5] have found that CO_2 can be transformed into methanol in a photocatalytic reaction. Methanol is an important chemical and convenient liquid fuel.

One crucial constraint on solving the problem of CO_2 is that any energy source used should not produce more CO_2. Solar energy is one of the best choices because it is clean and inexhaustible. However, the quantum efficiency is so far very low. Huynh et al. [6] reported a solar power conversion efficiency of only 10% in conventional inorganic solar cells; the most advanced but expensive cell has an efficiency of 30%. Moreover, 95% of solar light reaching ground is visible light [7,8]. Consequently, highly efficient photoreduction of CO_2 is preferentially desired.

Previous work [2] revealed that the optimum copper loading was 2 wt% due to the highest Cu dispersion. The best operation conditions for CO_2 photoreduction, including CO_2 pressure, weight of catalysts, and addition of NaOH, have been studied. This work aims to extend the fundamental understanding of the relationships among the sol–gel procedure, the properties of catalysts, and photocatalytic activity. The preparation parameters, such as the copper precursors, adding times, and posttreatments, are under investigation. This understanding can eventually be applied to develop visible-light-responsive photocatalysts, and to control the products selectivity of photoreaction using solar energy.

* Corresponding author.
E-mail address: cswu@ntu.edu.tw (J.C.S. Wu).

0021-9517/$ – see front matter
doi:10.1016/j.jcat.2003.09.002

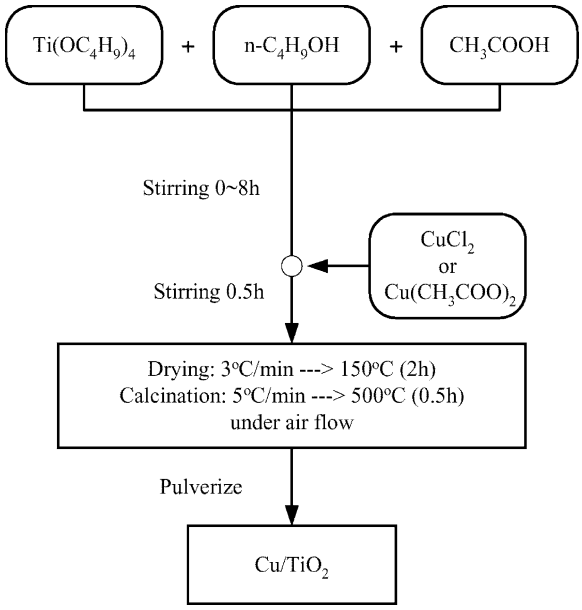

Fig. 1. Schematic of improved sol–gel procedure.

2. Experimental

2.1. Preparation of Cu/TiO_2 catalysts

An improved sol–gel process was used to synthesize copper-loaded titania photocatalysts. Fig. 1 depicts the procedure. Titanium butaoxide, *n*-butanol, and acetic acid were vigorously stirred in a beaker in a temperature and humidity-controlled glove box. Copper precursor was added during the above hydrolysis and polycondensation period. The resulting transparent green sol was dried at 150 °C and calcined at 500 °C in flowing air. The catalyst was then pulverized. Different adding periods, ranging from 0 to 8 h, and copper precursors, either copper chloride or copper acetate, were used. The procedure is detailed in a previous work [1]. Additionally, posttreatments of the resultant catalysts before reaction were also investigated. The H_2 reduction conditions were carried out at 300 °C for 3 h in a 5% H_2/Ar flow. For comparison, two commercial titania, Merck and Degussa P25, were deposited or impregnated by either the photodeposition (P) or the incipient wetness (I) method to make Cu/P25 and Cu/Merck catalysts, respectively. Table 1 summarizes the preparation conditions and the abbreviated forms of the prepared catalysts.

2.2. Characterization

The specific surface area of the catalyst was measured by N_2 adsorption using a Micrometrics ASAP 2010. A diffuse reflectance UV–vis spectrophotometer (Hitachi, U3410) was employed to obtain the UV–vis spectrum. The crystalline phase was identified by X-ray diffractometry (XRD) on a MAC (M03XHF, Material Analysis and Characterization, Japan). X-ray photoelectron spectroscopy (XPS) was performed using a VG Microtech MT500 with an Mg-K_α X-ray source. All binding energies were referenced to oxygen (1s) at 530.7 eV or carbon (1s) at 285.6 eV. A scanning electron microscope (SEM), equipped with an energy-dispersive spectrometer (EDS) LEO 1530 FEG–SEM–EDS, was used to observe the morphology of the catalyst and to measure its elemental ratio. The element distribution was analyzed by measuring the X-rays emitted after an exciting electron beam (15 keV) scanned a small area of a compressed catalysts pellet. In the temperature-programmed reduction (TPR) experiments, a quartz sample holder was loaded with approximately 0.1 g of fresh catalysts. The sample was heated from room temperature to 500 °C in a 5% H_2/Ar stream. A flow rate of 30 ml/min and a heating rate of 10 °C/min were used in all TPR experiments.

The X-ray absorption spectra (XAS) of the Cu and Ti K edge for all catalysts were measured at the Wiggler 17C station of the Taiwan Synchrotron Radiation Center in Hsinchu Science-based Industrial Park. A fluorescence mode was used to make the XAS measurement of a small amount of titania-supported copper catalyst. The powder sample was pressed in a sample holder positioned at 45° to the incident X-ray beam in a sample box. The fluorescent X-rays from the sample passed through a Ni filter and reached the detector. The filter was used to avoid the interference from other atoms or incident X-rays. The measurement of titanium was in transition mode directly. The X-ray photon energy varied across and beyond the absorption edge of the measured atom. For Cu, it was in the range from 200 eV below the copper absorption edge at 8979 to 800 eV above it. The intensity of both fluorescent (I_f) and incident (I_o) X-rays was measured to calculate the absorption coefficient (μ) for the

Table 1
Preparation conditions of copper-loaded titania photocatalysts

Sample	Procedure	Cu (wt%)	Copper precursor	Adding time (h)	Posttreatment
$CuCl_2$-*x* h	Sol–gel	2	$CuCl_2$	$x = 0$–8	None
$CuAc_2$-*y* h	Sol–gel	2	$Cu(CH_3COO)_2$	$y = 0, 8$	None
r-$CuCl_2$-*x* h	Sol–gel	2	$CuCl_2$	$x = 0$–8	H_2 reduction
r-$CuAc_2$-*y* h	Sol–gel	2	$Cu(CH_3COO)_2$	$y = 0, 8$	H_2 reduction
Cu/Merck	P[a]	< 2	$CuCl_2$	–	None
Cu/P25	I[b]	2	$CuCl_2$	–	None

[a] P: photodeposition method.
[b] I: incipient wetness method.

atoms of interest using the equation, $\mu x = I_o/I_f$, where x is the thickness of the sample. Spectral analysis followed the standard steps of background correction and normalization, before the near-edge absorption structure was determined. Moreover, the spectra of pure Cu_2O, CuO powder, and Cu foil were measured as standard references.

Generally, XAS can be divided into two types of structures superimposed on an X-ray absorption edge. The first structure is the X-ray absorption near-edge structure (XANES), which pertains to energies up to around 50 eV above the absorption edge. The second one extends from around 50 eV above the absorption threshold to several hundred eV above it, and is known as the extended X-ray absorption fine structure (EXAFS). These two kinds of spectra in this work were derived from the WinXAS 2.33 software [9].

Catalyst particles were first spread in distilled water and pumped into a capillary cell to measure zeta potential. Laser beams illuminated the particles in the capillary cell to generate their electrophoretic mobility. The Zeta Sizer, Malvern $2000HS_A$, recorded the electrophoretic mobility and then related to the Henry equation resulting in the zeta potential as a function of pH value. A pH value ranging from 5 to 12 was applied by adjusting the amount of NaOH added; each pH measurement was made five times.

2.3. Photoreduction of CO_2

The experiment was carried out in a cylindrical quartz reactor with a capacity of 300 ml. A weight 0.3 g of catalyst powder was suspended in 0.2 N NaOH solution. This condition was optimal according to a previous study [2]. Ultrapure CO_2 from Air Products and Chemicals was bubbled through the reactor for at least 4 h to ensure that all dissolved oxygen was eliminated; then, the irradiation lamp was turned on to start the photoreaction. The illumination system included a mercury lamp (Ultra-Violet Products Inc., USA; 11SC-1), either UVC (254 nm) or UVA (365 nm), in the center of the reactor. The whole system was tightly closed during the irradiation. The temperature, pH value, and dissolved oxygen concentration were monitored continuously. A needle-type probe was inserted into the reactor to withdraw a small liquid sample. After catalyst particles were filtered, the sample was analyzed using a GC-equipped flame ion detector and a 2-m-long Porapak Q column. Analytical results indicated that methanol was the major hydrocarbon.

3. Results

3.1. Characteristics of catalysts

From the previous study [2], 2 wt% Cu/TiO_2 catalyst yielded the highest methanol under a 6-h UVC irradiation. In this study, all the copper loadings of the catalysts were maintained at about 2 wt% to investigate other effects. The XRD spectra indicate only the anatase phase of titania, and

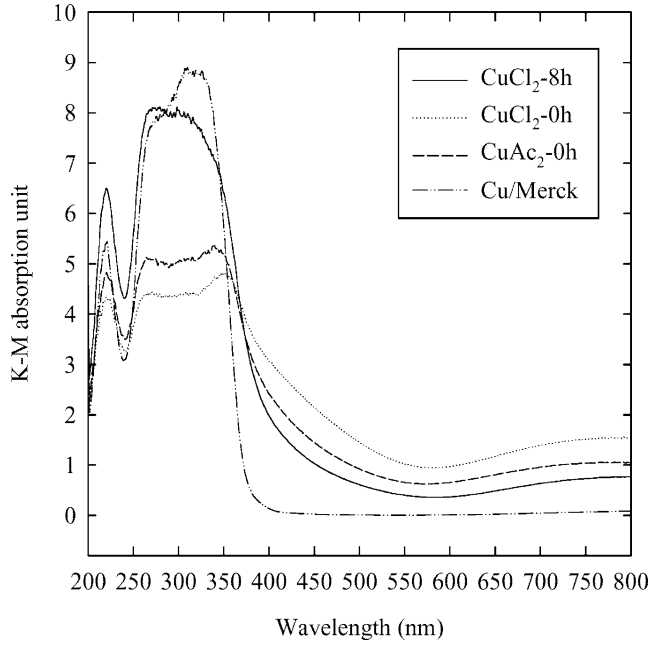

Fig. 2. UV–vis spectra of Cu/TiO_2.

no significant peaks related to copper phases for any sol–gel-derived Cu/TiO_2. The sizes of crystals estimated from the Scherrer equation were all about 20 nm. Different sol–gel procedures did not result in notably different XRD or BET results. The BET surface areas of all the catalysts ranged from 20 to 30 m^2/g and were less than that of pure TiO_2, 63 m^2/g. The "$CuAc_2$-8 h" catalyst was an exception, with a surface area of 67 m^2/g, similar to that of pure TiO_2. The micropores of the catalysts were identified from the N_2 adsorption isotherms. Fig. 2 displays the UV–vis spectra that show the influence of copper on the UV–vis absorption. For pure titania (Merck), the absorption is associated with the excitation of the O 2p electron to the Ti 3d level [10]. The absorption edge extends to longer wavelengths for Cu/TiO_2, revealing good contact between TiO_2 and Cu grains [11].

Fig. 3 shows the results of XPS spectra of 2 wt% Cu/TiO_2 prepared from various procedures. Because of small Cu loading and high photoionization cross section [12], reference spectra of copper particles, Cu_2O and CuO, are also shown in Fig. 3 to identify the copper state on the surface of TiO_2. The Cu (2p)-binding energies of Cu_2O were found to be 932.8 and 952.8 eV, respectively. However, the binding energies for CuO were 1 eV above those for Cu_2O, at 933.8 and 953.8 eV, respectively. According to the position and the shape of the peaks, regardless of various procedures, the copper on the surface of TiO_2 may exist in multiple-oxidation states but Cu(I) is the primary species even after H_2 reduction.

Table 2 presents the quantitative analysis calculated from the XPS. For 2 wt% Cu loading, the bulk Cu/Ti molar ratio was calculated to be about 0.026, but the quantitative analysis revealed much higher Cu/Ti ratios, estimated from the XPS. XPS can only detect the outer most surface ($\sim$ 10 nm)

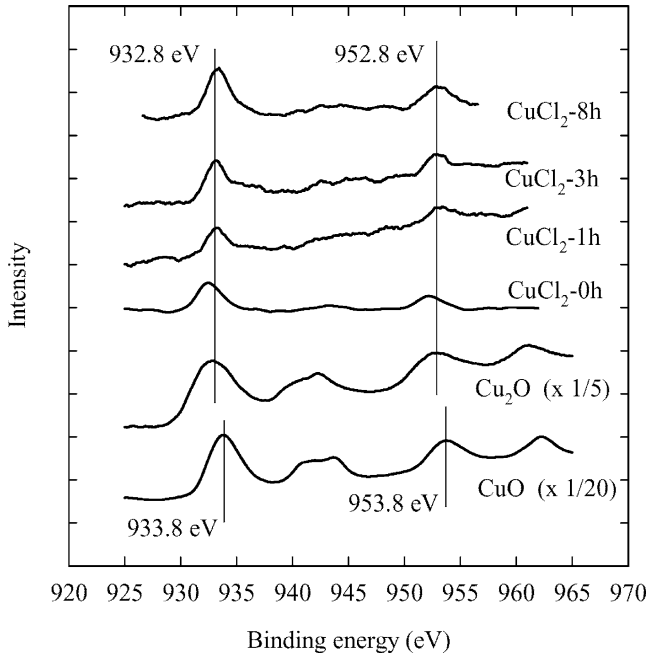

Fig. 3. XPS Cu(2p) spectra of 2% Cu/TiO_2 and Cu standards.

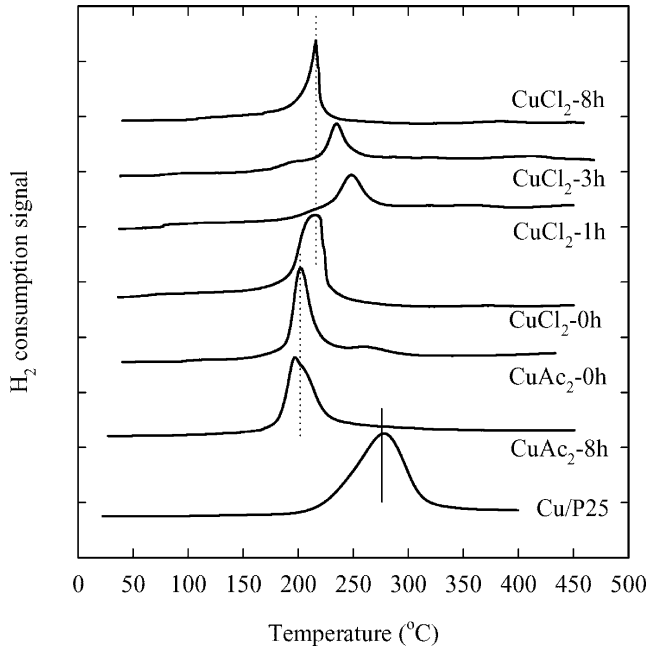

Fig. 4. TPR results of 2% Cu/TiO_2.

Table 2
Specific surface area, crystallize size, and relative Cu/Ti molar ratio of 2% Cu/TiO_2[a]

Sample	Surface area	Crystallize size[b]	Cu/Ti	
	(m^2/g)	(nm)	XPS	EDS
$CuCl_2$-0 h	25	22	0.116	0.035
$CuCl_2$-1 h	24	21	0.046	0.043
$CuCl_2$-3 h	25	23	0.080	0.054
$CuCl_2$-8 h	26	20	0.119	0.041
r-$CuCl_2$-1 h	–	–	–	0.050
r-$CuCl_2$-3 h	–	–	–	0.042
r-$CuCl_2$-8 h	28	21	0.240	0.036
$CuAc_2$-0 h	28	23	0.064	0.038
$CuAc_2$-8 h	67	24	0.068	0.036
r-$CuAc_2$-0 h	–	–	–	0.035
r-$CuAc_2$-8 h	–	–	–	0.067
Cu/Merck	10	48	0.187	–

[a] The bulk Cu/Ti molar ratio was calculated to be 0.026.
[b] Estimated from the Scherrer equation.

of a sample. The results indicate that copper was dispersed mostly on the surface of the prepared catalysts. The substitution of copper chloride to copper acetate reduced the Cu/Ti ratio. The catalyst $CuCl_2$-1 h had the lowest Cu ratio on the surface. For comparison, the Cu/Merck catalyst prepared by the photodeposition method had all copper particles on its surface.

The quantitative analysis of the elements in catalysts was also estimated by EDS analysis. Table 2 also presents relative bulk Cu/Ti molar ratio from EDS. The electron energy (15 keV) of the EDS can detect elements near 1 μm in depth from a sample surface. The results indicate that these values are slightly larger than the calculated bulk value of 0.026. When $CuCl_2$ was used as a copper precursor, detectable Cl remained in the catalysts. Chlorine resided in the catalysts even after calcination or H_2 reduction. The molar ratio of Cl was calculated based on the area of peaks from EDS. The amount of residual Cl was found to be affected by the adding time of $CuCl_2$ during the hydrolysis period. The Cl molar ratio reached a maximum $\sim 0.6\%$ when $CuCl_2$ was added between 1 and 3 h of hydrolysis. Posttreatment by H_2 reduction at 300 °C for 3 h only eliminated small amount of Cl.

Fig. 4 plots the TPR results of 2 wt% Cu/TiO_2. Pure titania did not consume H_2 in this temperature range. The hydrogen reduction temperatures (T_R) of prepared catalysts via various sol–gel procedures were all near 200 °C. Precursor $CuAc_2$ had T_R 20 °C lower than that of $CuCl_2$. However, when copper chloride was added at either 1 or 3 h, a higher T_R was required to reduce these two catalysts. Furthermore, the area under their peaks was smaller than the areas under those of other sol–gel-derived Cu/TiO_2. The TPR of the catalyst used for comparison, Cu/P25 prepared via the incipient wetness method, showed a reduction peak at 280 °C but the area under its peak was larger than the areas under those of all sol–gel-derived Cu/TiO_2.

The XANES of CuO, Cu_2O, and Cu standards were measured for comparison with other samples. A preedge was clearly observed for Cu_2O and Cu standards. For CuO standard, the absorption edge was slightly shifted to higher photon energy. Cu standard gave a split near-edge spectrum. In Fig. 5, results for catalysts with different amounts of copper loading were compared to the Cu XANES spectra. The major Cu(I) oxidation state was concluded according to the absorption edge. A higher Cu loading corresponded to a clearer preedge, especially at a loading above 2 wt%. Catalysts with higher Cu loading appeared to exhibit the characteristic split copper peak. Higher loading resulted in the aggregation of

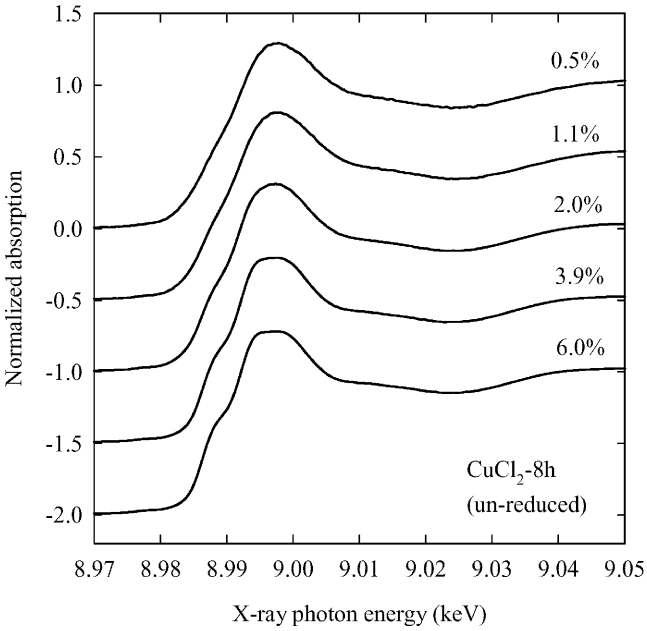

Fig. 5. Effect of Cu loading (%) on XANES spectra.

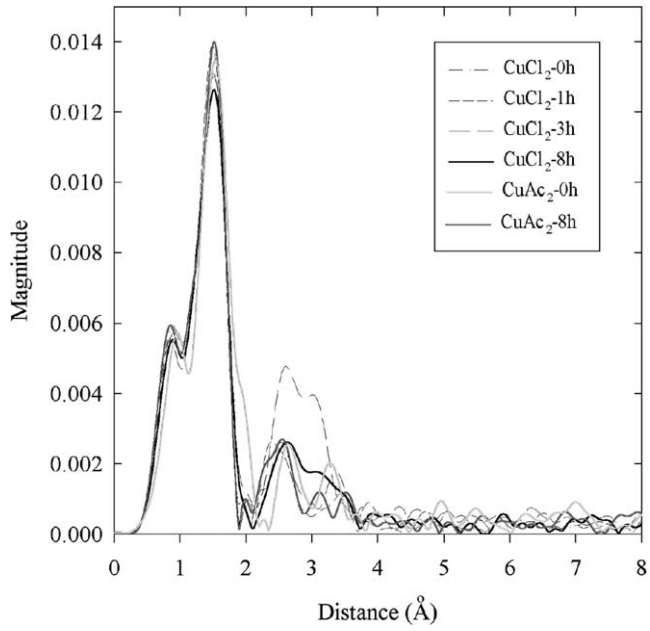

Fig. 7. Effect of $CuCl_2$ or $CuAc_2$ adding times on FT-EXAFS spectra.

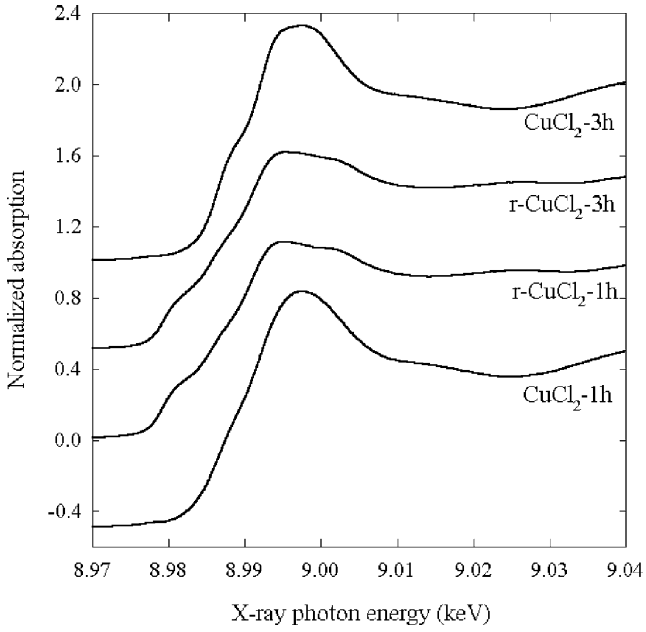

Fig. 6. Effects of H_2 reduction on XANES spectra of $CuCl_2$-1 h and $CuCl_2$-3 h catalysts.

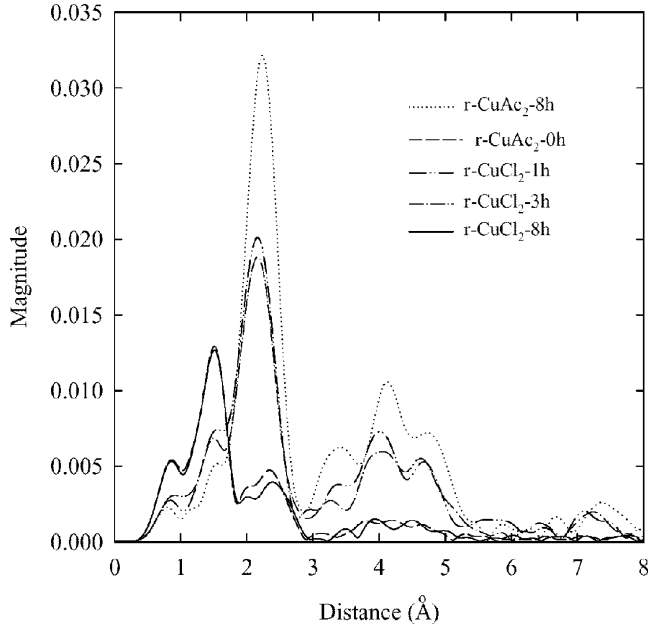

Fig. 8. Effects of precursors and adding times on Fourier transform (FT) EXAFS spectra for reduced 2% Cu/TiO_2.

copper particles and decreased copper dispersion. A copper X-ray diffraction peak of 6 wt% Cu/TiO_2 was also observed in a previous study due to aggregation under high Cu loading [2].

Fig. 6 displays the XANES spectra of catalysts prepared with differented $CuCl_2$ adding time and the effect of H_2 reduction. The position and shape of the absorption edge contributed to the Cu(I) absorption. In addition, Fig. 6 shows some distinguished results. The absorption spectra of $CuCl_2$-1 h and $CuCl_2$-3 h dramatically changed after H_2 reduction. The major oxidation state of Cu changed to Cu(0). However, whether or not H_2 reduction had occurred, the structures of $CuCl_2$-0 h and $CuCl_2$-8 h were similar.

The FT-EXAFS spectra of CuO, Cu_2O, and Cu standards were compared with Figs. 7–9. Fig. 7 displays the effects of various periods of adding $CuCl_2$ or $CuAc_2$ on the FT-EXAFS spectra of Cu/TiO_2. Cu(I) particles exhibit two main geometries. One is isolated Cu(I), in which the Cu–O peak is located at around 1.5 Å, and the other is aggregated Cu(I), which contributes to a Cu–O–Cu peak at around 2.6 Å [13,14]. Most of the copper on these catalysts was well-dispersed Cu(I) small particles, resulting in

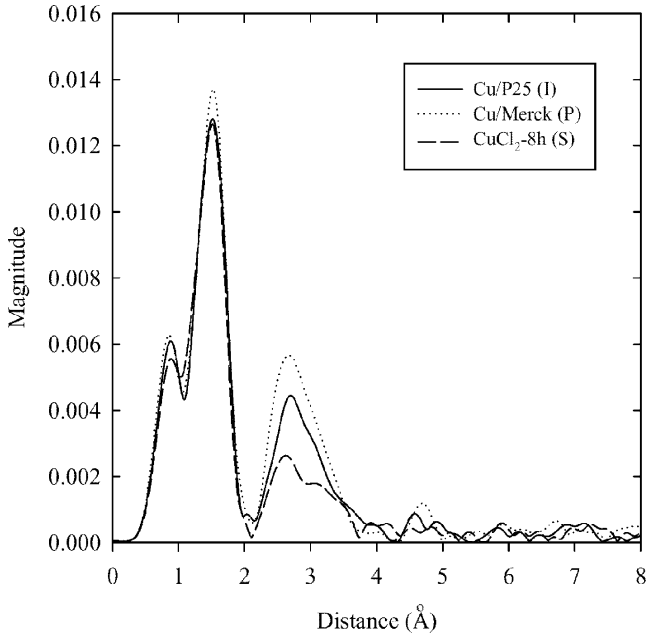

Fig. 9. Effect of preparation methods on FT-EXAFS spectra. (I, incipient wetness; P, photoreduction; S, sol–gel).

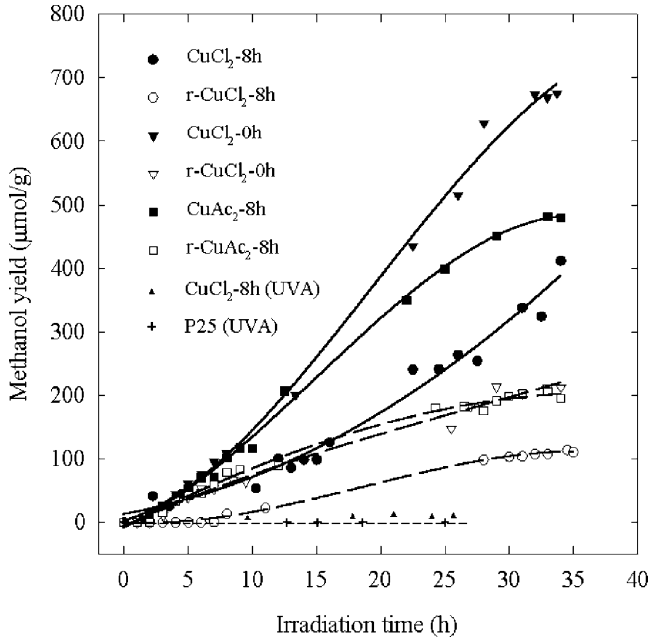

Fig. 10. Photocatalytic activity of 2% Cu/TiO_2 under UVC (254 nm) or UVA (365 nm) illumination.

a major peak at 1.5 Å. Except for $CuCl_2$-3 h catalyst, a very few aggregated Cu_2O (at 2.6 Å) or CuO (at 2.5 Å) particles formed on $CuCl_2$-0 h, $CuCl_2$-1 h, and $CuCl_2$-8 h. Fig. 8 is the FT-EXAFS spectra showing the effect of H_2 reduction. The H_2 reduction only slightly influenced $CuCl_2$-0 h and $CuCl_2$-8 h catalysts, the Cu structures of which were similar to that of the well-dispersed isolated Cu(I) particle, even after H_2 reduction treatment. However, lots of Cu(I) particles were reduced to Cu(0) on $CuCl_2$-1 h and $CuCl_2$-3 h catalysts, resulting in a characteristic peak at 2.2 Å [14,15].

Another copper precursor of $Cu(CH_3COO)_2$ was used to prepare 2 wt% Cu/TiO_2 catalysts. Fig. 8 shows the major characteristic peak of r-CuAc-0 h at 1.5 Å, to which the isolated Cu(I) particles contributed. However, the reduced r-$Cu(Ac)_2$-8 h gave most Cu(0) species resulting in a major peak at 2.2 Å.

Fig. 9 compares the FT-EXAFS spectra for three preparation methods using $CuCl_2$ precursor. The spectra indicate that 2 wt% Cu/TiO_2 by these methods all resulted in isolated Cu(I) particles. However the sol–gel method still gave less Cu aggregation (a smaller peak at 2.6 Å) than other methods.

The surface potential of a catalyst is a major factor that controls the stability of its aqueous suspension. The point of zero charge (pzc) is a critical pH value in an aqueous solution. At this pH value, the charge on particles is zero and the particles favorably aggregate. Particles can be well dispersed at either higher surface potential or the working pH value far from the pzc. The catalysts particles were suspended in an aqueous solution during the photocatalytic reaction. The influence of pH value on zeta potential was studied for various catalysts. The isoelectric point of most copper-loaded titania in distilled water is below pH 7, similar to that of pure TiO_2 and Degussa P25. Within this pH range, all catalysts, except $CuCl_2$-0 h and $CuAc_2$-8 h, carried negative zeta potential, indicating that their surface was negative. The zeta potentials of $CuCl_2$-0 h and $CuAc_2$-8 h catalysts were positive at pH 7.

3.2. Photocatalytic activity

Fig. 10 presents the CO_2 photoreduction results for various catalysts. Methanol yield was used to evaluate the performance of the catalysts since it was the major hydrocarbon product. After 30 h of UVC (254 nm) irradiation, the best four catalysts were, in order, $CuCl_2$-0 h, $CuAc_2$-8 h, $CuCl_2$-8 h, and $CuAc_2$-0 h, with a maximum methanol yield above 600 $\mu mol/g_{catal}$. The H_2-reduced catalysts would decrease the methanol yields. An increase wavelength of UV significantly decreased the methanol yield. The methanol yields were only in the range of 10 $\mu mol/g_{catal}$ under 30 h of irradiation with a UVA (365 nm) lamp, as shown in Fig. 10. The production of methanol by commercial TiO_2 (Degussa P25) under UVA irradiation was undetectable.

3.3. Sol–gel process

Fig. 11 plots the time dependence of pH and temperature during the sol–gel process, indicating that the variation of temperature changes. In the sol–gel process used herein, titanium butaoxide was mixed in sequence with butanol and acetic acid. Initially, the temperature of titanium butaoxide was about 28 °C; then the temperature quickly increased to 35 °C as two solutions were mixed in. Thereafter, the temperature fell to 31 °C within 1 h, increasing again to nearly

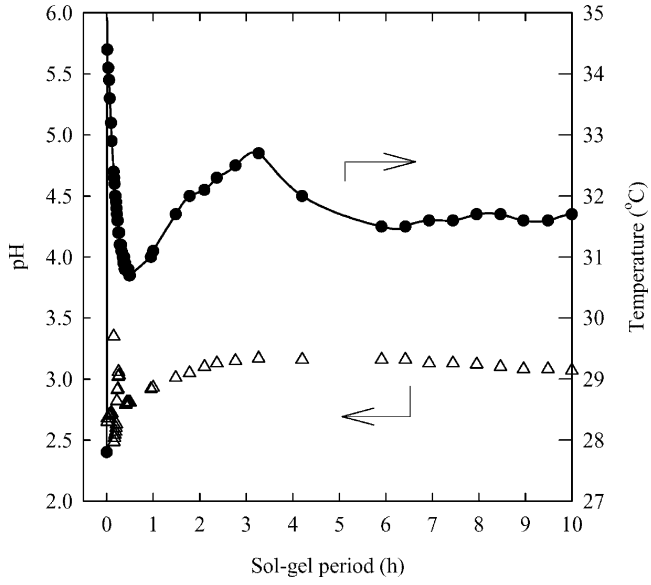

Fig. 11. Variation of pH and temperature during the sol–gel process.

33 °C in the third hour. Finally the temperature monotonically decreased and remained stable at near 31.5 °C to the end of the hydrolysis.

4. Discussion

4.1. Copper state and dispersion

The catalytic activity of Cu/TiO_2 in CO_2 photoreduction was related to the preparation and properties of the catalysts. The XPS results in Fig. 3 show that the shape and the position of the Cu 2p-binding energy indicated a combination of Cu(II), Cu(I), and Cu(0) states. Cu(I) was the primary chemical species. Moreover, the difference between the quantitative analysis results obtained by XPS and those obtained by EDS, shown in Table 2, indicates that Cu was near the surface because of the much higher Cu/Ti ratio in the XPS results.

A comparison of Cu absorption edge and near-edge structure between standards and catalysts gave additional evidence of the major Cu(I) state on the catalysts. Furthermore, the extended XAS data analysis elucidated the environments of the Cu atoms. The major peaks in the EXAFS spectra, at 1.5 and 2.2 Å, are characteristic of the isolated Cu(I) and Cu(0) particles, respectively. Aggregated Cu(I) also contributes partially to a peak at 2.6 Å. The derived atomic contribution to the X-ray absorption peak at 2.6 Å indicates notable aggregation of copper particles in the catalysts. Most copper in the catalysts was stable in Cu(I) status after calcination, and some even after H_2 reduction. That is, although copper particles on TiO_2 existed in multiple oxidation states, the isolated Cu(I) dominated.

The characterization also revealed the difference between the extents of copper aggregation. The choice of $CuCl_2$ and the addition at either the beginning or the final stage of the sol–gel process would lead to a better dispersion of Cu particles and the stability of the Cu(I) state. Bokhimi et al. [11] suggested that the strong interaction between copper and titania causes the high dispersion of copper. They found that a $CuCl_2$ precursor led to well-dispersed Cu at low loading. The choice of $CuAc_2$ as a Cu precursor also yielded good dispersion but poor Cu(I) stabilization. As shown in Fig. 8, a large amount of Cu(I) was reduced to Cu(0) in the $CuAc_2$-8 h catalyst after H_2 reduction; similar results were obtained for $CuCl_2$-1 h and $CuCl_2$-3 h catalysts.

The copper particles on the catalysts, $CuCl_2$-1 h and $CuCl_2$-3 h, were easily aggregated and easily reduced to Cu(0), as shown in Fig. 8. This finding is consistent with the XPS quantity analysis in Table 2, that indicates that the Cu/Ti ratios of the well-dispersed catalysts, $CuCl_2$-0 h and $CuCl_2$-8 h, exceeded those of other catalysts. Furthermore, the T_R of $CuCl_2$-1 h and $CuCl_2$-3 h were higher and peak areas were smaller than those of other catalysts. The copper acetate precursor led to worse Cu dispersion than $CuCl_2$, which exhibited a lower Cu/Ti ratio in Table 2, and yielded a weaker interaction between Cu and TiO_2 networks.

The sol–gel procedure can synthesize the Cu/TiO_2 catalysts with good Cu dispersion and isolated Cu particles. As shown in Fig. 9, the peak height at 2.6 Å was the least for the sol–gel-derived catalyst, $CuCl_2$-8 h. Less aggregation of copper particles was obtained by the sol–gel method than by impregnation or photodeposition. The aggregation of Cu particles also led to a higher T_R than those of $CuCl_2$-1 h (250 °C) and $CuCl_2$-3 h (240 °C) shown in Fig. 4. Catalysts derived by impregnation and photodeposition gave even higher T_R, at about 280 °C. The interaction between Cu and TiO_2 was stronger for sol–gel-derived catalysts than catalysts derived by impregnation or photodeposition. A catalyst using copper acetate led to a stronger Cu–TiO_2 interaction than that using $CuCl_2$, as evident by the lower T_R in Fig. 4. Boccuzzi et al. [16] believed that during wet impregnation, copper ions coordinated to oxygen atoms on TiO_2 and formed an amorphous surface phase. The easy reduction of the Cu/TiO_2 catalysts obtained in a sol–gel process can be explained by the fact that the sol–gel process yields well-dispersed and small copper particles [16,17]. The aggregated Cu would increase the T_R of $CuCl_2$-1 h and $CuCl_2$-3 h.

4.2. Effects of sol–gel procedure on copper state

Either $CuAc_2$ or $CuCl_2$ precursor added at the beginning with titania sol yielded similar resultant Cu states, that is, of well-dispersed small Cu(I) particles. Adding $CuCl_2$ at the end of hydrolysis yielded no significantly different results from those adding it at the beginning, while significant differences arose adding it within 1 to 3 h of hydrolysis. When $CuCl_2$ was added at 1 or 3 h, a high T_R was required to reduce both catalysts. Furthermore, the areas of their peaks were smaller than those for other sol–gel-derived Cu/TiO_2.

Some copper was presumed to be covered by the TiO_2 surface [17].

Fig. 11 plots the temperature and pH during the sol–gel process. The first high-temperature peak was associated with the exothermic esterification of butanol and acetic acid. The water released by esterification was then progressively consumed by in the hydrolysis of titanium butaoxide, which is an endothermic reaction, so the temperature decreased gradually. Extra butanol was released during the hydrolysis so that further esterification proceeded, consuming acetic acid. Consequently, the temperature increased again and the pH value increased until the third hour. The composition of the solution at different times changed the solubility and distribution of the copper precursor. $CuCl_2$ added between 1 and 3 h could not be uniformly dispersed so the Cu dispersion of the resultant Cu/TiO_2 on the surface was poorer and the interaction with TiO_2 was weaker. This fact also explains why the H_2 could further reduce Cu(I) to Cu(0), resulting in the aggregation of Cu. Furthermore, the lower Cu dispersion and the weaker interaction caused more residual Cl to remain in the catalysts and increased the H_2 reduction temperature (T_R), as shown in Fig. 4.

4.3. Major factors controlling CO_2 photoreduction

Under the conditions for CO_2 photoreduction applied in this work, adding NaOH at the beginning of the reaction resulted in a pH value of 12. After CO_2 was bubbled into the solution, saturated solubility was reached and the pH value dropped to 7. All catalysts in the reaction solution were far away from the pzc and were well dispersed. Comparing the variation of zeta potential within this range, most catalysts carried a negative zeta potential, indicating that the surfaces of the catalysts, except $CuCl_2$-0 h and $CuAc_2$-8 h, were negative. $CuCl_2$-0 h and $CuAc_2$-8 h had a positive zeta potential at pH 7.

In Fig. 10, the catalysts that performed well in CO_2 photoreduction under UVC irradiation were in the order $CuCl_2$-0 h, $CuAc_2$-8 h, and $CuCl_2$-8 h, which was also consistent with the positive zeta potential at pH 7. The positive zeta potential indicated positive surface charge on the surface of a catalyst. The positive surface enhanced the adsorption of carbonate ions and strengthened the interaction between TiO_2 and Cu, improving the photoactivity [7,17]. The surface area of $CuAc_2$-8 h was higher than that of any other catalyst (Table 2) and was believed to facilitate its performance. The photoactivity decreased somewhat after H_2 reduction. Based on the FT-EXAFS results, the relative amount of Cu(I) decreased after H_2 reduction. Therefore, the active sites for CO_2 photoreduction were isolated Cu(I) species. However, the Cu(0) state might also induce the production of other hydrocarbons, as revealed by some experimental results.

5. Conclusions

In this work, the specific surface area and the UV–vis spectra were similar for all investigated catalysts. In our improved sol–gel process and under calcination conditions, small copper particles can be well dispersed on the surface of anatase titania. Copper loaded on the surface enhanced the photoactivity. According to XAS and XPS analysis, the oxidation state of Cu(I) was suggested to be the active species for CO_2 photoreduction. Higher copper dispersion and smaller copper particles on the titania surface correspond to a greater improvement in the performance of CO_2 photoreduction. The greater the aggregation of copper particles, the higher the H_2-reducing temperature required and the larger amount of chlorine resided on catalysts. The choice of a $CuCl_2$ precursor increased the Cu dispersion over that obtained with a copper acetate precursor. The post H_2 reduction only slightly affected the Cu oxidation state and caused little aggregation of any sol–gel-derived catalyst, except in the case of any catalyst for which a Cu precursor was added at an inappropriate time during hydrolysis. A positive zeta potential at pH 7 promotes the photoactivity of CO_2 photoreduction.

Methanol was favorably produced on Cu/TiO_2 catalysts in an aqueous solution of CO_2 under UV irradiation. The transformation of photo to chemical energy by a catalyst provides a more efficient way than performed by green plants. The results demonstrate that the improved sol–gel method is a promising technique for preparing such photocatalysts.

Acknowledgments

The authors thank the National Science Council of Taiwan, the Republic of China, for financially supporting this research under Contract NSC-90-2214-E-002-038. The authors also thank Dr. Jyh-Fu Lee of the Wiggler 17C station of the Taiwan Synchrotron Radiation Center and Ms. Chaoling Lai of the Surface Analysis Lab at the National Taiwan University for their effort in instrumental analysis.

References

[1] J.C.S. Wu, I-H. Tseng, W.-C. Chang, J. Nanoparticle Res. 3 (2001) 113.
[2] I-H. Tseng, W.-C. Chang, J.C.S. Wu, Appl. Catal. B 37 (2002) 37.
[3] B. Aurian-Blajeni, M. Halmann, J. Manassen, Solar Energy 25 (1980) 165.
[4] K. Hirano, K. Inoue, T. Yatsu, J. Photochem. Photobiol. A Chem. 64 (1992) 255.
[5] H. Yamashita, H. Nishiguchi, N. Kamada, M. Anpo, Res. Chem. Intermed. 20 (1994) 815.
[6] W.U. Huynh, J.J. Dittmer, A.P. Alivisatos, Science 295 (2002) 2425.
[7] A.L. Linsebigler, G. Lu, J.T. Yates Jr., Chem. Rev. 95 (1995) 735.
[8] M. Anpo, Y. Ichihashi, M. Takeuchi, H. Yamashita, Res. Chem. Intermed. 24 (1998) 143.
[9] T. Ressler, J. Synch. Rad. 5 (1998) 118.

[10] A. Fuerte, M.D. Hernández-Alonso, A.J. Maíra, A. Martinez-Arias, M. Fernández-García, J.C. Conesa, J. Soria, J.G. Munuera, J. Catal. 212 (2002) 1.
[11] X. Bokhimi, A. Morales, O. Novaro, T. López, O. Chimal, M. Asomoza, R. Gómez, Chem. Mater. 9 (1997) 2616.
[12] J.C. Vickerman, Surface Analysis—The Principle Techniques, 1st ed., Wiley, New York, 1997, p. 64.
[13] M. Anpo, M. Matsuoka, K. Hanou, H. Mishima, H. Yamashita, H.H. Patterson, Coordin. Chem. Rev. 171 (1998) 175.
[14] T. Liu, Y.N. Xie, T.D. Hu, Nucl. Instrum. Methods Phys. Res. B 160 (2000) 301.
[15] V.V. Kriventsov, O.V. Klimov, O.V. Kikhtyanin, K.G. Ione, D.I. Kochubey, Nucl. Instrum. Methods Phys. Res. A 448 (2000) 318.
[16] F. Boccuzzi, A. Chiorino, G. Martra, M. Gargano, N. Ravasio, B. Carrozzini, J. Catal. 165 (1997) 129.
[17] X. Bokhimi, O. Novaro, R.D. Gonzalez, T. López, O. Chimal, A. Asomoza, R. Gómez, J. Solid State Chem. 144 (1999) 349.